Available online at www.sciencedirect.com

ScienceDirect

Procedia CIRP 74 (2018) 353–356

www.elsevier.com/locate/procedia

10th CIRP Conference on Photonic Technologies [LANE 2018]

Laser surface tempering of hardened chromium-molybdenum alloyed steel

Carlos Soriano[a,]*, Goretti Alberdi[a], Jon Lambarri[a], Ana Aranzabe[a], Armando Yáñez[b]

[a]*Ik4-Tekniker, Iñaki Goenaga 5, 20600 Eibar, Spain*
[b]*Universidade da Coruña, Escola Politécnica Superior, 15403 Ferrol, Spain*

* Corresponding author. Tel.: +943206744 ; Fax: +943206744; E-mail address: Carlos.soriano@tekniker.es

Abstract

The effect of a laser tempering process, subsequent to a laser hardening treatment, on the microstructure, microhardness, structural composition of phases and residual stresses of a 42CrMo4 steel has been studied. The tempering process has been carried out using a 10 kW diode laser and a galvanometer scanner head. Results show that the subsequent tempering process, after the laser hardening treatment, can be a complementary and effective method to adjust, through the selection of the appropriate process parameters, the desired degree of hardness and tensional state of the processed area, attending to the specific requirements demanded in a component.

Keywords: laser tempering; martensite; tempered martensite; retained austenite; $42CMo_4$.

1. Introduction

Tempering is a widespread heat treatment in industry. This process is normally carried out on previously surface or bulk hardened martensitic steel components for reducing fragility, increasing ductility, toughness and relieving its tensile stress state. In addition, tempering leads to a reduction in hardness and mechanical strength.

Surface tempering treatment using induction heating technology is also common in industry, especially for medium and high carbon steels, cast iron and some alloys [1]. This process is typically carried out after the hardening treatment, using the same technology, in order to reduce the brittleness of the material associated to the previous quenching, through the reduction of the retained austenite concentration, and the high hardness.

In the case of laser technology, tempering has received less attention. The process consists of heating by the action of a laser beam, below the austenitic transformation temperature, the surface of a previously hardened steel. Compared to the traditional tempering process, heating and cooling take place in a very short time, producing a softening of the previous martensite structure, and generating a greater toughness and lower hardness phase, consisting mainly of tempered martensite.

Tempering of overlapped laser hardening single tracks has been one the most studied topics so far [3,4]. On the other hand, work carried out by Gureev et al. related to the laser tempering process before and after a surface hardening treatment, using CO_2 lasers on different steels, is also significant [5,6]. Other investigations have focused on the laser tempering treatment to reduce the fragility of certain surface hardened or nitrided regions subjected to high dynamic loads [7], as well as on the study of the tempering process of hypereutectoid steels to increase their machinability through a controlled reduction of the surface hardness [8]. Recently, several studies have appeared concerning laser tempering treatments on industrial components, such as the research carried out by Järvenpää et al. [9] related to the local surface softening of high-strength steels, to improve their forming properties of car body parts, and as the study carried out by Leunda et al. [10], focused on the secondary hardening process through laser tempering treatment of powder tool steels coatings applied by laser cladding.

10.1016/j.procir.2018.08.140

The present work focuses on the study of the laser tempering process of a previously surface hardened 42CrMo4 steel, as an alternative to surface tempering treatments that are applied to different industrial components such as shafts and gears among others, through more conventional processes.

2. Methodology

A 56 mm in diameter and 200 mm in length cylindrical bar, previously turned, from 42CrMo4 medium alloyed carbon steel were used in this study. The chemical composition of the alloy is shown in Table 1. The material was previously normalized, presenting a typical ferrite-perlite structure, with a hardness of 173 HB and a G7 grain size characterized according to ASTM 112 standard.

Table 1. Chemical composition (wt. %) of the treated material.

	C	Mn	P	S	Si	Cr	Mo
42CrMo4	0.400	0.820	0.017	0.010	0.330	1.020	0.160

A continuous wave 10 kW high power diode laser was used in the research, using two of the four emission wavelengths available, 910 nm and 940 nm, with a maximum possible power of 2500 W each. The laser beam was lead to the working area through a 1 mm circular fibre optic followed by a 72 mm and 600 mm collimating and focusing optics respectively. The optical beam path was completed with a two-dimensional scanning head able to produce in the focal plane, through the movement of galvanometric mirrors, an equivalent spot of 25.8 x 7.8 mm. The head was fixed to a 6-axis robot capable of positioning the equivalent laser spot over the area of interest. In addition, the cylindrical rod specimen was clamped to an indexing table.

To carry out the study, a battery of individual laser track tests was programmed in the radial direction of the cylindrical bar. Every test was composed by two stages, a first single revolution stage of hardening, carried out at an angular speed of 0.27 rad/s and an average power density of 1705 W/cm^2, followed, after 45 s, by a tempering stage, performed over the previous hardened region, in which the average power density of every test was varied from 265 W/cm^2 to 1705 W/cm^2 in steps of 160 W/cm^2, maintaining an angular speed of 0.48 rad/s.

The geometry, grain size and microstructure of the processed areas were characterized by optical and scanning electron microscopy. The samples were polished with diamond powder and chemically etched in a 4% Nital solution. Microhardness measurements were performed by means of a microhardness tester with a load of 0.3 Kg from the material surface to the core, every 0.1 mm.

Qualitative measurement of the phase composition, as well as surface residual stresses of the treated region in each test were measured by a parallel beam X-ray diffractometer, using an irradiated area of 2 mm in diameter and Cr radiation, operating at 40 kV and 40 mA. Surface residual stresses were measured in the longitudinal direction of the processed steel cylinder every 3 mm, from the central region of the hardened track area to the unaffected area of the material, using the $(211)_\alpha$ X-ray diffraction peak located at $2\theta \sim 156º$.

3. Results and discussion

3.1. Microstructure and structural composition of phases

The treated regions present different microstructures depending on the power density used and the temperature reached in the material. Fig. 1a shows the cross section of the test carried out at 1065 W/cm^2, as a representative example of the performed treatments. The temperature generated at 265 W/cm^2 was not enough to transform the original microstructure, which presents lath martensite precipitated during the cooling cycle. From 425 W/cm^2 to 1065 W/cm^2, a tempered martensite microstructure in the processed regions is observed, formed by an aggregate of fine carbides dispersed in a ferritic matrix, with the presence of retained austenite, as can be seen, as example, in Fig. 2, corresponding to the tempering treatment carried out at 905 W/cm^2. From 1065 W/cm^2, as the temperature increases, a martensite microstructure appears again in the regions near the surface, due to the heat generated above the austenizing critical temperature, and finally, below this region, tempered martensite is observed due to the gradual decrease in temperature from the surface into the material, as shown in Fig. 1b.

On the other hand, the grain size of the processed areas was G7, remained unaltered respect to the characterized value of the original material.

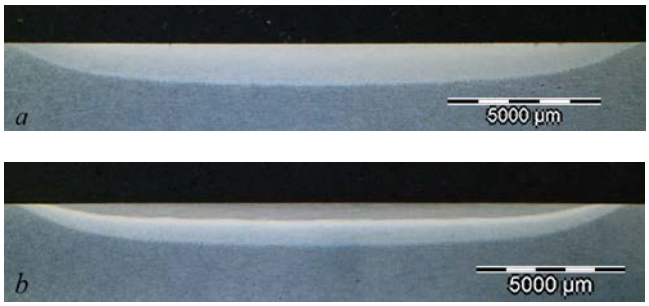

Fig. 1. Cross sections of the laser processed area at (a) 1065 W/cm^2 and (b) 1385 W/cm^2.

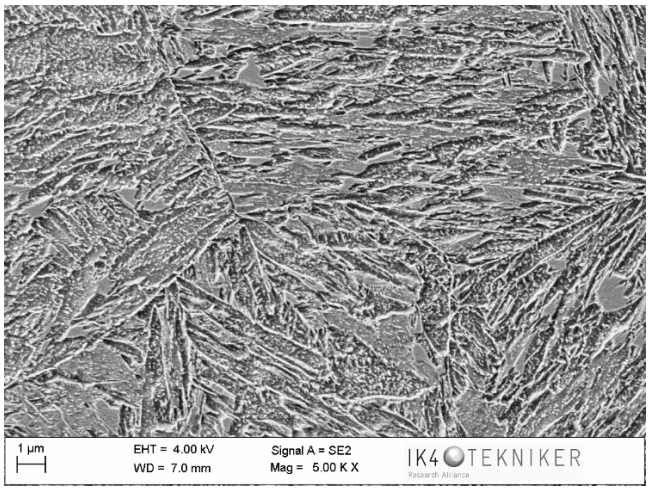

Fig. 2. Resulting microstructure after the laser tempering treatment using a power density of 905 W/cm^2.

Fig. 3 shows the X-ray diffraction scans of the surface region treated in each of the tests performed. The diffraction peaks corresponding to the planes $(111)_\gamma$, $(200)_\gamma$ and $(220)_\gamma$, being the maximum intensity peak the crystallographic plane $(111)_\gamma$, are shown. These peaks are typical of a face-centered cubic structure (fcc), characteristic of an austenitic microstructure, which mainly indicates the presence of retained austenite, both in hardened and tempered regions, resulting the volumetric fraction of austenite very similar in all of them.

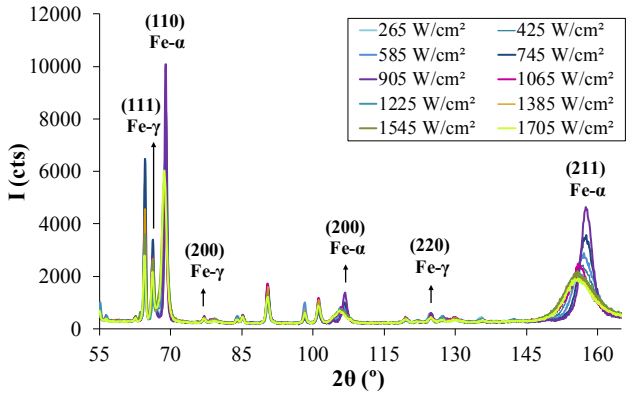

Fig. 3. X-ray diffraction scans of the 42CrMo4 treated regions.

Moreover, in Fig. 3, are also represented the X-ray diffraction scans of the crystallographic planes $(110)_\alpha$, $(200)_\alpha$ and $(211)_\alpha$, which indicates the presence of body-centered cubic (bcc) crystalline structures, corresponding to the ferritic microstructure of the base material, the martensite and the tempered martensite of the treated regions, with different degrees of intensity. Martensite and tempered structures can be distinguished by the displacement of the centres of gravity of the diffraction peaks corresponding to α-Fe, due to the modification of the parameters of the crystalline network during the tempering process and therefore to the loss of the tetragonality of the network of the martensitic structure generated after the hardening process. This effect is shown in Fig. 4, where the diffraction peaks of the plane $(211)_\alpha$ of the treated regions are represented. The results show a gradual increase in the tempered martensite phase as the treatment temperature increases, being the highest fraction of tempered martensite corresponding to the treatment performed at 905 W/cm^2. As the power density increases, once the austenizing temperature is exceeded, the diffraction lines gradually move slightly towards smaller angles to the base metal diffraction peak, indicating the presence of martensite according to the microstructure results previously shown.

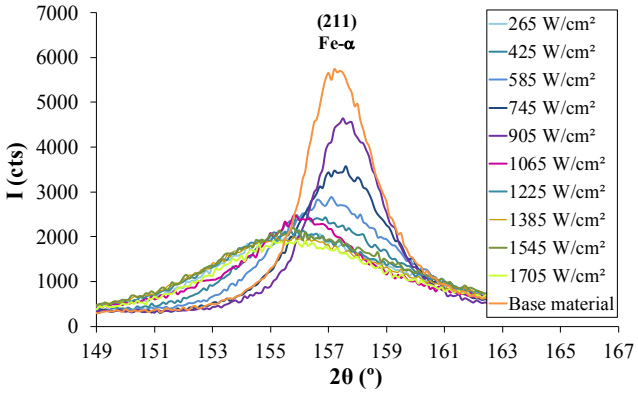

Fig. 4. X-ray diffraction scans of the 42CrMo4 treated regions corresponding to the $(211)_\alpha$ crystallographic plane.

3.2. Hardness

As mentioned before, the laser tempering treatment produces a softening of the previous martensite microstructure, reducing the hardness of the irradiated areas. This effect can be clearly observed in Fig. 5, where micro-hardness values obtained for each test, from the surface to the core of the material, are shown. At 265 W/cm^2, the hardness remains at values close to 650 HV, meaning that practically no tempering temperatures have been reached, keeping the treated region the typical martensite structure originated after the laser hardening operation. However, from 425 W/cm^2, as the power density used increases and therefore the temperature in the treated area, the hardness decreases gradually until reaching around 400 HV for a power density of 1065 W/cm^2.

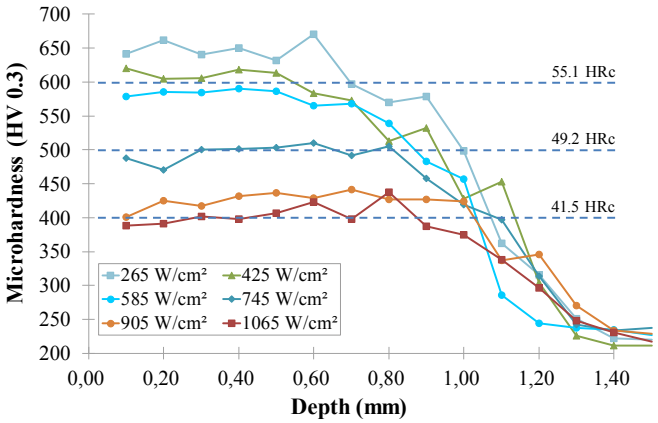

Fig. 5. Microhardness profiles across the processed area for tests of 265 to 1065 W/cm^2.

On the other hand, using higher power densities, as shown in Fig. 6, microhardness of the areas near the surface increases again, as a result of the austenization of the microstructure and subsequent martensitic transformation carried out during the cooling cycle, followed by a region of lower hardness, which corresponds to a microstructure of tempered martensite, according to the results shown in the previous sections.

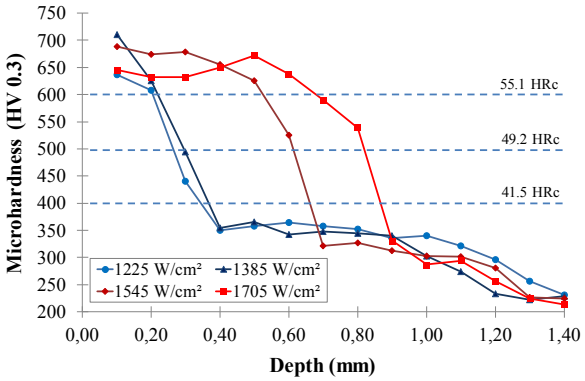

Fig. 6. Microhardness profiles across the processed area for tests of 1225 W/cm^2 to 1705 W/cm^2.

3.3. Residual stresses

Fig. 7 and Fig. 8 show longitudinal tensile stresses measured in the surface of every processed region at power density levels from 265 to 1065 W/cm^2 and 1225 to 1705 W/cm^2 respectively. According to the results shown above, at 265 W/cm^2 the heating has been insufficient to transform the initial structure of martensite, and therefore the obtained residual stresses are compressive. As the power density increases, residual stresses growth gradually, being still compressive at 425 W/cm^2, were the tempered temperature has been low. However, at higher power density levels residual stresses become tensile, reaching its maximum value in the case of tests carried out at 745 W/cm^2 and 905 W/cm^2, in which, according to the previous results, tempered martensite fraction is high. From 1065 W/cm^2, where the tempering temperature is high, close to the critical austenizing temperature, residual stresses become compressive again, reaching at the central processed surface region values below -200 MPa. As shown in Fig. 8, and according to the achieved microhardness and X-ray diffractive scan results, at higher power density levels the residuals stresses become compressive on the surface regions again, agreeing with the martensite microstructure shown above.

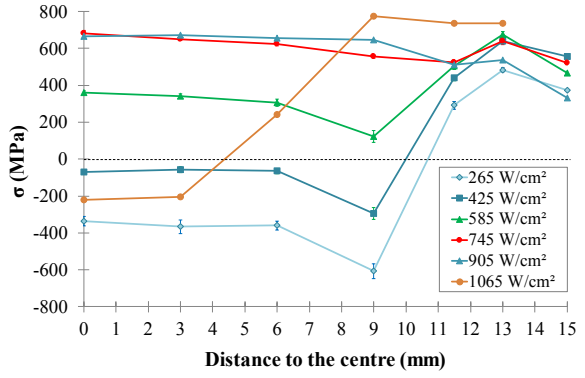

Fig. 7. Surface longitudinal residual stresses measured for test of 265 W/cm^2 to 1065 W/cm^2.

Finally, it should be noted that maximum residual stresses have been concentrated in the transition zones between the hardened region and the untreated material, as can be seen in Fig. 7 and Fig. 8, starting at 9 mm from the central processed area, due mainly to the balance established between the tensile and compressive residual stresses generated in the material.

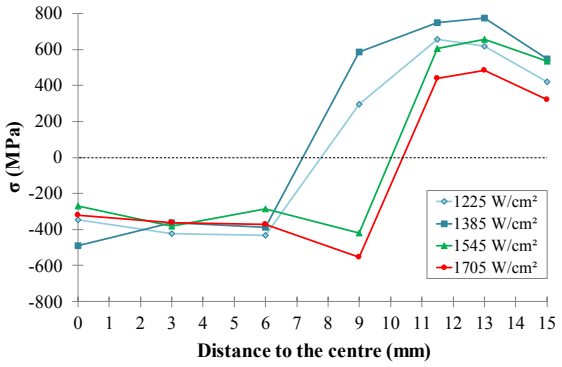

Fig. 8. Surface longitudinal residual stresses measured for tests of 1225 W/cm^2 to 1705 W/cm^2.

4. Conclusions

The effect of laser tempering process carried out on a previously laser hardened region, on the microstructure, microhardness, structural composition of phases and residual stresses of 42CrMo4 steel has been studied. The experimental results achieved show that the laser tempering treatment transforms the martensite hardened phase into a tempered martensite one, being a complementary and effective method to adjust, through the selection of the appropriate values of power density and interaction time, the desired degree of hardness as well as tensional state of a processed area, in order to meet the requirements demanded in a given component.

References

[1] Rudnev V, Loveless D, Cook RL. Handbook of induction heating. 2nd ed. Boca Raton: CRC Press; 2017.
[2] Burakowski T, Wierzchon T. Surface engineering of metals: principles, equipment, technologies. Boca Raton: CRC Press; 1999.
[3] Hegge HJ, De Beurs H, Noordhuis J, De Hosson JThM. Tempering of Steel during Laser Treatment. Metall. Trans. A 1990;21:987-995.
[4] Lakhkar RS, Shin YC, Krane MJM. Predictive modeling of multi-track laser hardening of AISI 4140 steel. J Mater Sci Eng A 2008;480:209-217.
[5] Gureev DM, Mednikov SI. Combination of laser quenching and tempering for hardening tool steels. Sov J Quantum Electron 1988;18:1054-1057.
[6] Gureev DM, Mednikov SI, Shukhostanov VK, Yamshchikov SV. Influence of laser tempering on the characteristics of surface layers of tool steels. Sov J Quantum Electron 1990;20:1003-1006.
[7] Guriev VA, Tesker EI. Laser treatment of parts with stress raisers. Met Sci Heat Treat 1991;33:172-174.
[8] Raghavan S, Melkote SN, Hashimoto F. Laser tempering based turning process for efficient machining of hardened AISI 52100 steel. J Manuf Process 2013;15:318-328.
[9] Järvenpää A, Jaskari M, Hietala M, Mäntyjärvi K. Local laser heat treatments of steel sheets. Phys Procedia 2015;78:296 – 304.
[10] Leunda J, García Navas V, Soriano C, Sanz C. Effect of laser tempering of high alloy powder metallurgical tool steels after laser cladding. Surface & Coatings Technology 2014;259:570–576.